

1 **Predicting performance of in-situ microbial enhanced oil recovery process and**
2 **screening of suitable microbe-nutrient combination from limited experimental**
3 **data using physics informed machine learning approach**

4 Sree Pavan^a, K. Arvind^b, B. Nikhil^b, P. Sivasankar^{a,*}

5 ^a Geo-Energy Modelling & Simulation Lab, Department of Petroleum Engineering,
6 Indian Institute of Petroleum & Energy, Visakhapatnam - 530003, India.

7 ^b Department of Mechanical, Chemical and Electronics Engineering,
8 OsloMet University, Oslo, Norway

9 *Corresponding author

10 Contact Details of Corresponding Author (P. Sivasankar)

11 Email ID: sivasankar.petro@iipe.ac.in

12 Ph: 91 9600043460

13

14

15

16

17

[Original Research Article]

18

Submitted to

19

Bioresource Technology

20

January 2022.

21 **Abstract**

22 To screen/identify suitable microbe, nutrient and reservoir for successful field
23 implementation of in-situ MEOR technique, it is important to predict the oil recovery
24 and quantify the relative importance of influencing parameters from limited
25 experimental data. For this purpose, Physics-Informed Machine Learning (PIML)
26 approach is adopted in this study, which is developed by integrating the physics-based
27 and Machine Learning (ML) models. It is found that biosurfactant yield *w.r.t* nutrient
28 (Y_{PS}), flow velocity and initial oil saturation (S_{oi}) are correspondingly the most
29 influential microbial kinetic, operational and reservoir parameters. Higher oil recovery
30 is achieved by selecting a microbe-nutrient-reservoir pair having higher Y_{PS} and S_{oi}
31 values but with lower Y_{XS} (microbial yield *w.r.t* nutrient) value. Among 12 ML models
32 analysed, Neural network model had predicted the oil recovery relatively accurate ($R^2 \sim$
33 0.98). Overall, this PIML approach helps to devise strategies for maximizing oil
34 recovery at initial laboratory stage itself with limited experimental data.

35 **Keywords:** Microbial Enhanced Oil Recovery; Machine Learning; Biosurfactants;
36 Modelling; Kinetics

37 **1. Introduction**

38 To meet the increase in global energy demand and to sustain crude oil
39 production from depleting oil reservoirs, more than half of the crude oil that is left after
40 primary and secondary recovery techniques must be recovered by suitable Enhanced Oil
41 Recovery (EOR) techniques (Joshi et al., 2016). In relative to existing chemical EOR
42 methods, In-situ Microbial Enhanced Oil Recovery (MEOR) method is an economical
43 and environmental friendlier EOR technique (Joshi et al., 2016; Varjani and Upasani,

2016; Shibulal et al., 2018; Jeong et al., 2022). In in-situ MEOR process, exogeneous (or) indigenous microbes are injected into the reservoir, which subsequently undergoes metabolic activity within the reservoir by utilizing nutrients and producing bioproducts, which consequently helps to recover the crude oil from the reservoirs (Joshi et al., 2016; Varjani and Upasani, 2017; Shibulal et al., 2018; Markande et al., 2021). Though in-situ MEOR technique inherits several advantages, it is not widely implemented in the field across the globe as other chemical EOR techniques due to the existence of following challenges (Nikolova and Gutierrez, 2020): (a) complexity in predicting the oil recovery performance of in-situ MEOR technique; and (b) lack in quantifying the relative importance of each influencing parameter on final oil recovery. Resolving these challenges at initial lab investigation stage itself will correspondingly: help to decide whether to implement in-situ MEOR technique in the given reservoir or not and to identify/screen the suitable microbe-nutrient-reservoir combination for attaining better oil recovery; and assist in development of strategies for optimizing the oil recovery.

To evaluate the oil recovery performance of in-situ MEOR process, earlier, several core flooding experimental studies (Joshi et al., 2016; Varjani and Upasani, 2016; Shibulal et al., 2018) and physics based computational modelling studies (Nielsen et al., 2016; Sivasankar and Kumar, 2016, 2017, 2019; Jeong et al., 2021, 2022) were performed. However, performing core flooding experimental studies to identify/screen a suitable microbe-nutrient-reservoir combination from several available combinations makes experimental approach an expensive and time-consuming exercise. Though physics-based models can provide better prediction of oil recovery with physically consistent results, but it is computationally intensive to perform uncertainty quantification and optimization studies as it requires to solve the non-linear equations

68 for several simulation runs (Thanh et al., 2020; Karniadakis et al., 2021). Moreover, it is
69 also unfeasible to quantify the relative importance of each influencing parameter on oil
70 recovery by both experimental and physics-based modelling approach as it requires
71 several experiments. Recently, Machine Learning (ML) models/algorithms are
72 increasingly used for different bioprocess applications to predict and optimize its
73 performance (Cruz et al., 2012; Tang et al., 2021; Zhang et al., 2021; Wang et al.,
74 2022). With the availability of large input and output datasets, ML models can quickly
75 predict the outcome of complex problems and quantify the relative importance of each
76 input parameters, which is otherwise difficult by using only physics-based models
77 (Thanh et al., 2021; Tang et al., 2021). However, with the limited availability of data
78 from experimental and field studies, it will not be feasible to apply ML
79 models/algorithms alone as it may predict physically inconsistent results with lesser
80 accuracy. Hence the requirement to have a quick and physically consistent results from
81 limited observed/experimental data with better accuracy is achieved by integrating both
82 the physics informed model and data driven ML model into a single hybrid model
83 called Physics Informed Machine Learning (PIML) model (Thanh et al., 2020;
84 Karniadakis et al., 2021). In recent times, PIML modelling approach is gaining
85 popularity because of its ability to accommodate the merits of both physics-based model
86 and ML model in a single model, while mitigating their respective drawbacks. Recently,
87 PIML modelling approach have been successfully used for different applications (Thanh
88 et al., 2020; Karniadakis et al., 2021; Liu et al., 2021). However, the use of PIML
89 approach for in-situ MEOR application have not been explored yet at least to the
90 authors knowledge.

91 SOMETHING ABOUT PIML WRITE ABOUT EXPLAINABILITY,
92 INTERPRETABLE AND PHYSICALLY CONSISTENT...

93

94

95 Hence the novelty of the present work is in introducing the PIML approach for in-situ
96 MEOR application to predict its oil recovery performance and to quantify the relative
97 importance of parameters influencing the oil recovery using limited experimental data.
98 In particular, the objectives of the present work are: (a) to develop a framework to
99 integrate the physics based model and ML model into a single PIML model for
100 generating a large, relevant and physically consistent data sets from limited
101 experimental data; (b) to quantify the relative importance of each parameter on
102 influencing the final oil recovery using PIML approach, and subsequently to identify the
103 critical kinetic and operational parameters influencing the oil recovery; and (c) to
104 identify the suitable ML model among 12 different ML models that shall be used
105 directly in PIML approach for predicting the oil recovery performance.

106 The present PIML approach study will help the end-users: to quickly select a
107 favourable microbial-nutrient-reservoir combination from several other available
108 options; to decide whether to implement in-situ MEOR technique in a particular
109 reservoir or not; and to devise operational strategies for maximizing the oil recovery.

110 **2. Materials and Methods**

111 In the present study, PIML approach is developed by combining the physics-
112 based model and ML model into a single model. Initially, laboratory experiments are
113 performed to determine the microbial kinetic and reservoir properties data. Based on

114 these limited experimental data, physics-based models for microbial kinetic and oil
115 recovery processes are developed. From these physics-based models, large, physically
116 relevant input and output data sets are generated. Using these large datasets, the ML
117 models are then trained and tested to quantify the relative importance of each parameter
118 and to predict the oil recovery quickly. The methodology for developing this PIML
119 approach is presented in detail in this section and briefed in Figure 1.

120 [Figure 1]

121 ***2.1 Classification and collection of input parametric data***

122 In the present study, 13 input parameters are considered. The corresponding
123 values of these input parameters constitutes the input parametric data. In the present
124 study, the input parametric data are classified as: (i) microbial kinetic parametric data,
125 (ii) operational parametric data, and (iii) reservoir parametric data, based on the
126 corresponding properties of microbes, nutrients, operational and reservoir conditions.

127 ***2.1.1 Collection of input microbial kinetic parametric data from experimental studies***

128 In the present study, the microbial kinetic parameters that are considered as
129 input are maximum microbial growth rate [U_{max} , (h^{-1})], yield of microbes *w.r.t* sucrose
130 (Y_{XS}), yield of biosurfactants *w.r.t* sucrose (Y_{PS}) and Monod half saturation coefficient
131 (K_{XS} , (gl^{-1})). The corresponding values of these microbial kinetic parameters are
132 considered as input microbial kinetic parametric data. In the present study, the input
133 data for all these microbial kinetic parameters are sourced from the experimental studies
134 of Sivasankar et. al., 2016, in which, *Pseudomonas putida* MTCC 2467 was used as
135 microbe, while sucrose and ammonium sulphate were used as carbon and nitrogen
136 source nutrient, respectively. In that study, at pH 8 condition, experiments on microbial

137 growth, nutrient utilization and biosurfactant production were carried out to determine
138 the values of microbial kinetic parameters for predicting the oil recovery.

139 *2.1.2 Collection of input operational and reservoir parametric data*

140 In the present study, the operational parameters that are considered as input are
141 mean flow velocity of injection fluid within reservoir [$u, (mh^{-1})$], viscosity of injection
142 fluid [$\mu_w, (Nhm^{-2})$], initial/injection concentration of microbes [$X_i, (gl^{-1})$],
143 initial/injection concentration of sucrose [$S_i, (gl^{-1})$], initial/injection concentration of
144 ammonium sulphate [$A_i, (gl^{-1})$], and resident time [$T_r, (h)$]. These input operational
145 parameters are controlled by the operators/scientists in the field/laboratory during the
146 implementation of in-situ MEOR technique. Finally, the reservoir fluid-rock parameters
147 that are considered as input parameters in the present study are initial residual oil
148 saturation [$S_{ori}, (fraction)$], irreducible water saturation [$S_{wir}, (fraction)$] and initial or
149 maximum oil-water Interfacial Tension (IFT) at the start of EOR [$\sigma_{max}, (mNm^{-1})$]. In
150 the present study, the input data for all these operational and reservoir rock-fluid
151 parameters are sourced from Sivasankar et al., 2016. Table 1 presents the sourced data
152 or reference value of all these input parameters. It is to be noted that for each input
153 parameter, only one reference value is available either from experiments or other
154 sources, which will be insufficient for applying the ML algorithms.

155 **[Table 1]**

156 *2.2 Generation of large input and output datasets from physics-based model*

157 In the present study, percent of oil recovery is the only parameter considered as
158 output parameter. This output oil recovery parameter is influenced by all the input
159 parameters (Sivasankar et al., 2016) that are mentioned in Tab. 1. In order to apply

160 Machine Learning (ML) algorithms for predicting the output oil recovery, large data
161 sets of input and output parameters are required to train and test the ML algorithms.
162 However, the availability of input and output parametric data from laboratory
163 experiments and other sources are limited (as presented in Tab. 1), which is inadequate
164 to implement the ML algorithms. Hence in the present study, large datasets of input and
165 output parameters are generated synthetically (data augmentation) for training and
166 testing the ML algorithms. Data augmentation is a mathematical method to synthesise
167 more data from the known (experimental) data when there is data insufficiency. The
168 methodology adopted in the present study for generation of input and output data is
169 similar to the method earlier adopted by Thanh et al., 2020, and it is outlined in sec.
170 2.2.1. and sec. 2.2.2.

171 *2.2.1 Generation of large input datasets from sourced reference values*

172 The reference value of input microbial kinetic parameters that are presented in
173 Tab. 1 are specific only to a particular temperature, pH, salinity, and pressure conditions
174 at which experiments were conducted. However, in actual reservoir fields, the reference
175 value of input parameters mentioned in Tab. 1 varies significantly due to the existence
176 of heterogeneity, resulting in uncertainty (Ansah et al., 2020; Thanh et al., 2020). Hence
177 accounting for this uncertainty, and to make the present model to be applicable for
178 wider variations in input parametric data during its field implementation, a 50%
179 Standard Deviation (SD) is considered to all the input parameter values (Thanh et al.,
180 2020). The resultant value range for each of these input parameters after considering the
181 SD is presented in Tab. 1. Subsequently, large datasets of about 10000 values (i.e., data)
182 for each of the input parameter is generated between their corresponding value range by
183 dividing it in equal intervals following the uniform distribution.

184 2.2.2 Generation of large output data sets using physics-based model

185 The output data on oil recovery is dependent on all the input parametric data.
 186 Hence, to generate the large data sets of output parameter (oil recovery, %) for training
 187 and testing of ML algorithms, the physics-based model (Eqs. 1- 8) (Sivasankar and
 188 Suresh Kumar, 2016) which is dependent on all input parameters is simulated several
 189 times using the generated input datasets. In the present physics-based model, the
 190 microbial kinetic model (Eqs. 1 – 4) simulates: growth kinetics of microbes (Eq. 1);
 191 nutrient utilization kinetics (Eq. 2); biosurfactant production kinetics (Eq. 3); and
 192 Monod’s kinetics (Eq. 4). While the oil recovery model (Eqs. 5 – 8) simulates: IFT
 193 reduction by produced biosurfactants (Eq. 5); increase in Capillary Number due to IFT
 194 reduction (Eq. 6); decrease in oil saturation due to increase in Capillary Number (Eq. 7);
 195 and the final percent of oil recovery (Eq. 8), which is the output and target data. Based
 196 on this obtained oil recovery data, performance evaluation of MEOR technique and
 197 screening of suitable microbe-nutrient-reservoir combination are carried out.

198 $dX/dt = \mu_x \cdot X$ (1)

199 $dS/dt = - \mu_x \cdot X/Y_{XS}; \quad dA/dt = - \mu_x \cdot X/Y_{XA}$ (2)

200 $dP/dt = (Y_{PS}/Y_{XS}) \cdot \mu_x \cdot X$ (3)

201 $\mu_x = U_{max} \cdot \{(S/K_{XS} + S) + (A/K_{XA} + A)\}$ (4)

202 $\log(\sigma^*) = \log(\sigma_{min}) + \log(\sigma_{max}/\sigma_{min}) \cdot \{(P - P_{max})/(P_{max} - P_{min})\}$ (5)

203 $N_{ca}^* = u_w \mu_w / \sigma^*$ (6)

204 $S_o = \left[\frac{-\tanh(v_1(N_{ca}^*) - v_3) + 1 + v_2}{-\tanh(v_1(N_{ca}^0) - v_3) + 1 + v_2} \right] S'_o \quad S_w = 1 - S_o$ (7)

205 $Oil\ recovery, \% = \{(S_w - S_{wir}) / (1 - S_{wir})\} \times 100$ (8)

206 In Eqs. (1 - 8), the terms: X , S , A and P represents the concentration of microbes,
 207 sucrose ammonium sulphate and produced biosurfactant, respectively in gl^{-1} ; μ_x
 208 represents the microbial growth rate in h^{-1} ; K_{XA} represents the half-saturation constant
 209 of ammonium sulphate in gl^{-1} ; Y_{XA} represents the yield of microbes *w.r.t* ammonium
 210 and sulphate, r ; Y_{PS} represents the yield of biosurfactant *w.r.t* sucrose; N_{ca} represents
 211 the updated IFT (mNm^{-1}) and Capillary Number, respectively; P_{min} and P_{max}
 212 represents the minimum and maximum biosurfactant concentration, respectively in
 213 gl^{-1} ; σ^* and σ_{min} represents the updated IFT and minimum IFT, respectively in
 214 (mNm^{-1}); S_o and S_w represents the saturation of oil and water, respectively in fraction;
 215 and v_1, v_2, v_3 are the constants.

216 By performing one simulation job of physics-based model from Eqs. 1 - 8, one
 217 output data on oil recovery is generated. Hence, in the present study, to generate a large
 218 database of output data, ten thousand (10000) simulation jobs were performed which
 219 resulted in generation of 10000 output data on % oil recovery. While, in each simulation
 220 job, the input value (data) of different input parameters that are required are sampled
 221 randomly from the generated input database using Latin Hyper-Cube Sampling (LHS)
 222 technique (Thanh et al., 2020). In some simulation jobs, the set of input data have not
 223 generated a valid positive output data (i.e., % of oil recovery), and such data are
 224 excluded from the training and testing of ML algorithms. Figure 2 shows the frequency
 225 distribution of all the input and output data values that were considered in the present
 226 study for training and testing of different ML algorithms.

227 [Figure 2]

228 ***2.3 Machine Learning Models***

229 Subsequent to the generation of large sets of input and output data, the
230 interaction strength (or) sensitivity of all 13 input parameters on the output oil recovery
231 is quantified by using Pearson Correlation Coefficient (PCC) and Spearman Rank
232 Corelation Coefficient (SRCC) values. PCC value measures the linear relationship
233 between two variables and SRCC value measures the monotonic relationship between
234 two parameters. Both PCC and SRCC values range from -1 to 1. Positive correlation
235 value between two parameters indicates that parameters are directly proportional, and
236 *vice versa*. Magnitude of the correlation indicates the strength of the relationship
237 between the two parameters. Higher the magnitude of correlation coefficient value,
238 higher is the association strength between the two parameters. Determination of PCC
239 and SRCC values helps to quantify the influence of different input parameters on output
240 oil recovery, which shall be used to screen the suitable microbes, nutrients and
241 reservoirs at the laboratory experimental stage for MEOR field implementation.

242 ***2.4 Prediction of relative importance score to quantify the significance of input*** 243 ***microbial kinetic, operational and reservoir parameters on output oil recovery***

244 In the present work, feature importance study is carried out to quantify the
245 relative importance of each input parameter on the output oil recovery using Random
246 Forest Classifier ML algorithm (Keprate and Ratnayake, 2019) in the present PIML
247 framework. This ML algorithm has been trained and tested using the input and output
248 parameter datasets that are generated from physics-based model (as described in sec
249 2.3). This feature importance study computes the Relative Importance (RI) score for
250 each input parameters in fraction, where its summation will be 1. Hence, RI score of an

251 input parameter quantifies the significance (or) importance of that input parameter on
252 influencing the output oil recovery in relative to other input parameters. Determination
253 of this RI score for all input parameters will help to identify the critical input
254 parameters influencing the output oil recovery, which subsequently guide the future
255 operation. In the present work, the results from the feature importance study would
256 help: (a) to identify the input parameters that are most and least important for
257 predicting the oil recovery, which subsequently helps to identify the input parameters
258 which exhibit higher and lower influence on the output oil recovery; (b) to identify the
259 critical input parameters that shall be optimized for improving the efficiency of oil
260 recovery; and (c) to determine the weightage functions of all input parameters, which
261 shall be used to screen the suitability of MEOR technique among other EOR techniques
262 and to identify the right combination of microbe-nutrient pair for attaining better oil
263 recovery during its field implementation.

264 ***2.5 Prediction and evaluation of different machine learning algorithms for MEOR*** 265 ***applications from lab data***

266 In the present study, Machine Learning (ML) model which is integrated within
267 the PIML approach is used to predict the output oil recovery. CRISP-DM methodology
268 was used for performing data mining and predicting the output oil recovery from input
269 parameters (Keprate and Ratnayake, 2019). The large data sets of input parameter data
270 and output data that are required for training and testing the ML model are sourced from
271 physics-based model which is embedded within the PIML approach (the procedure for
272 data generation using physics-based model is presented in sec. 2.2). As there are
273 different ML models available to do the prediction, it is necessary to identify the most
274 accurate and suitable ML model that can be used in the PIML approach by the end-users

275 (researchers/scientists in the laboratory) for predicting the oil recovery. Hence, in the
 276 present study, 12 different ML models/algorithms are used in the PIML approach to
 277 determine its accuracy in predicting the output oil recovery. The 12 different ML
 278 models/algorithms that were used in the present study are K-Nearest Neighbours
 279 (KNN), Decision Trees, Lasso, Ridge, Linear Regression, Random Forests, ADA Boost
 280 Regression, Gradient Boosting, Gaussian Process Regression, Polynomial Regression,
 281 Support Vector Regression (SVR) and neural networks.

282 For all these 12 ML models adopted in the PIML approach, the input parameter
 283 data was normalised, and was subsequently split into training data sets and test data sets
 284 in the ratio of 7:3 for training and testing of the ML model used. k-fold cross validation
 285 was performed on the training set by setting $k = 10$, and the best model is then evaluated
 286 on the test data set. In the present work, all the 12 ML models were trained using
 287 training data sets, and its prediction performance were compared based on 3 metrics,
 288 namely, Root Mean Square Error { $RMSE$; eq. (9)}, Coefficient of Determination { R^2 ;
 289 eq. (10)} and Explained Variance Score { EVS ; eq. (11)}.

$$290 \quad RMSE = \sqrt{\frac{\sum_{i=1}^n (y_i - \hat{y}_i)^2}{n}} \quad (9)$$

$$291 \quad R^2 = 1 - \frac{\sum_{i=1}^n (y_i - \hat{y}_i)^2}{\sum_{i=1}^n (y_i - \bar{y})^2} \quad (10)$$

$$292 \quad EVS = 1 - \frac{Var(y_i - \hat{y}_i)}{Var(y_i)} \quad (11)$$

293 In the Eqs. (9 - 11), where: y_i represents the actual % oil recovery determined from
 294 physics-based model; \hat{y}_i represents the predicted value of % oil recovery determined
 295 from ML model; \bar{y} represents the mean value of y_i ; n represents the number of
 296 samples; and Var represents the variance. $RMSE$ is a measure of accuracy, and lower

297 values indicate better fit of data. R^2 and EVS measures proportion to which a
298 mathematical model accounts for variation of a given data set. The ML model having
299 values of R^2 and EVS closer to 1 is the most accurate and suitable model that shall be
300 used to predict the % oil recovery for in-situ MEOR application.

301 **3. Results and Discussion**

302 ***3.1 Validation of physics based microbial kinetic model***

303 The validity of the physics-based microbial kinetic model that is used in the
304 present study is verified by comparing the present numerical model results with the
305 experimental data. From Fig. 3(a - c), it is observed that the present model results
306 (microbial, nutrient and bio-surfactant concentrations *w.r.t* time) is in good agreement
307 with the experimental data. As the present adopted model is validated, it is subsequently
308 used to generate large datasets.

309 [Figure 3]

310 ***3.2 Quantifying the influence of input parameters on output oil recovery***

311 [Figure 4]

312 Figure 4a shows the PCC and SPCC values in a matrix form that represents the
313 interaction (or) association strength between any two parameters involved in the MEOR
314 process. Fig. 4b specifically presents the PCC and SPCC values (i.e., interaction
315 strength) between all the input parameters with the output oil recovery parameter.
316 Results from Fig. 4a and Fig. 4b reveals that the input parameters, Y_{PS} , u , S_{ori} , μ_w , X_i ,
317 A_i , S_i , U_{max} , S_{wir} and T_r are directly proportional to the oil recovery, while the input

318 parameters K_{XS} , Y_{XS} and initial IFT are inversely proportional to the oil recovery.
319 These results are consistent with the reality, which validates the results shown in Fig. 4.

320 It is observed that among all these input parameters, the parameter, Y_{PS} had
321 strongly associated with the output oil recovery while compared to all the other input
322 parameters. This illustrates that the yield value of biosurfactants *w.r.t* sucrose (Y_{PS}) is
323 the dominant parameter that significantly influences the output oil recovery. Moreover,
324 it is also inferred that the oil recovery performance of MEOR process increases with
325 increase in Y_{PS} value, which means that with the increase in utilization of nutrients for
326 biosurfactant production, the oil recovery increases. This obtained result corroborates
327 with the earlier results of Sivasankar and Suresh Kumar, 2019, in which, it is reported
328 that Y_{PS} parameter significantly influences the oil recovery compared to other kinetic
329 parameters. From Fig. 4a and Fig. 4b, it is also observed that among the negatively
330 correlated input parameters (*i.e.*, parameters that are inversely proportional to the oil
331 recovery), Y_{XS} is the input parameter that is strongly associated with the output oil
332 recovery. This illustrates that lower the value of Y_{XS} (*i.e.*, less nutrient is utilized for the
333 growth of microbes), higher is the oil recovery. Hence, the study reveals that the higher
334 oil recovery is attained by selecting a microbe-nutrient pair that have higher value of
335 Y_{PS} and lower value of Y_{XS} . Based on these observations made on Y_{PS} and Y_{XS} values, it
336 shall be finally correlated that the ratio between Y_{PS} and Y_{XS} (*i.e.*, Y_{PS}/Y_{XS}) values for a
337 microbe-nutrient pair needs to be higher to achieve better oil recovery. Thus, based on
338 the determination of PCC and SPCC values, it is concluded that: (a) Y_{PS} and Y_{XS} are the
339 two input parameters that significantly influences the output oil recovery; and (b) oil
340 recovery could be maximized by selecting a microbe-nutrient pair having higher
341 Y_{PS}/Y_{XS} value at initial laboratory investigation stage itself.

342 ***3.3 Application of PIML approach for identifying critical input microbial kinetic,***
343 ***operational and reservoir parameters influencing the output oil recovery***

344 [Figure 5]

345 Figure 5a presents the Relative Importance (RI) score or relative strength of all
346 the 13 input parameters on influencing the output oil recovery. The RI score was
347 determined by performing feature importance study. As all the 13 input parameters
348 involved in the feature importance study were selected (or) sourced from the physics-
349 based model (Eqs. 1- 8), hence, all these input parameters are relevant and have some
350 influence on deciding the output oil recovery. This is evident from Fig. 5a, which shows
351 that each of the 13 input parameters have a non-zero RI score. Thus, in the present
352 PIML approach, all the 13 input parameters are considered for the training, testing, and
353 implementation of all ML algorithms (models) for predicting the output oil recovery.

354 It is observed from Fig. 5a that among all the input parameters, Y_{PS} has the
355 highest RI score of 0.168, hence, it is the most critical input which significantly
356 influences the output oil recovery. In order to exclusively understand the relative
357 importance of microbial, operational and reservoir parameters on deciding the output oil
358 recovery, correspondingly, Figs. 5b, 5c and 5d are plotted. It is understood from Fig. 5b
359 that among the input parameters that are related to microbes and nutrients (i.e., Y_{PS} , Y_{XS} ,
360 S_i , A_i , U_{max} , X_i , K_{XS}), Y_{PS} and Y_{XS} are relatively the most influential input parameters
361 with RI score of 0.168 and 0.1, respectively. While, K_{XS} is relatively the less significant
362 input kinetic parameter on deciding the percent of output oil recovery with RI score of
363 0.014. It is also observed from Fig. 5b that compared to injection concentration of
364 microbes, the injection concentration of nutrients (both, carbon and nitrogen source)

365 into the reservoir has relatively higher impact on deciding the output oil recovery. This
366 implies that for maximizing the oil recovery, continuous supply of nutrients to the
367 microbes need to be ensured for microbes to undergo metabolic activity within the
368 reservoir (*i.e.*, to produce biosurfactants) and recover the oil.

369 Fig. 5c shows the relative importance of operational parameters (u, μ_w, T_r) on
370 influencing the output oil recovery. It is observed from Fig. 5c that though all
371 operational parameters influence the output oil recovery, fluid velocity (u) is the input
372 operational parameter that influences the output oil recovery relatively more, and
373 closely followed by the viscosity of injection water (μ_w) parameter. This obtained
374 results are in accordance with the physics-based concept of Capillary Number, in which,
375 the viscous force (*i.e.*, product of u and μ_w) must be higher for achieving higher oil
376 recovery. Thus, the results from Fig. 5c implies that more oil could be recovered during
377 field implementation of in-situ MEOR technique by optimizing the injection velocity of
378 the microbial slug (*i.e.*, mixture of microbes, nutrients and water) and by increasing the
379 water viscosity using biopolymer producing microbes during in-situ MEOR application.

380 Figure 5d presents the relative importance scores of different parameters (*i.e.*,
381 $S_{ori}, S_{wir}, \sigma_i$) related to the fluids present within the reservoir. By correlating the results
382 from Fig. 5d and from Fig. 4b, it is inferred that among the fluid parameters, the initial
383 residual oil saturation parameter (S_{ori}) is the most significant parameter influencing the
384 oil recovery, and the oil recovery will be higher in reservoirs that has higher value of
385 S_{ori} . This finding is in good agreement with the earlier physics-based simulation studies
386 (Sivasankar et al., 2016) which states that the oil recovery performance increases with
387 the increase in initial residual oil saturation. Hence, based on this finding from Fig. 5d it
388 is suggested that the oil recovery performance of MOER technique could be improved if

389 the MEOR technique is implemented at an earlier stage of oil production (i.e., along
390 with secondary recovery stage), during which the oil saturation will be relatively higher
391 compared to the later stage (i.e., at tertiary recovery stage).

392 As the results presented in Fig. 5 (a – d) validates with the physics-based model
393 results, it has been affirmed that the physics has been infused into the ML model in the
394 present PIML approach. Hence the results obtained from this PIML approach can be
395 used to draw physical insights, based on which, suitable strategies can be developed for
396 maximizing the oil recovery.

397 ***3.4 Application of PIML approach to screen suitability of in-situ MEOR technique*** 398 ***and to identify suitable microbe-nutrient for in-situ MEOR implementation***

399 The RI score of each input parameter presented in Fig. 5a also correspondingly
400 represents the weightage factor of each input parameter. Based on this weightage factor,
401 the selection score of in-situ MEOR technique is calculated. This selection score helps
402 in initial screening of in-situ MEOR technique among other EOR techniques for field
403 implementation. The EOR technique that possess the highest selection score will be
404 considered further for field implementation. Earlier, the selection score for in-situ MEOR
405 technique was calculated based on the reservoir fluid and rock properties, and neglected
406 the consideration of microbial kinetic and operational parameters, which may mislead
407 the entire EOR screening process for field implementation. However, with the PIML
408 approach adopted in the present work, the selection score for in-situ MEOR technique is
409 calculated by including both microbial kinetic parameters (Y_{PS} , Y_{XS} , K_{XS}) and
410 operational parameters along with reservoir fluid and rock parameters. Thus, the present
411 work would enhance the accuracy in screening of in-situ MEOR technique, which

412 subsequently would help the end users to make better decision on selecting a suitable
 413 EOR for field implementation. The selection score for an EOR technique is calculated
 414 by using the formula, $Selection\ Score = \sum_{i=1}^n w_i a_i$. Here, i represents the input
 415 parameters; n represents the total number of input parameters; a_i represents the
 416 accuracy factor of input parameter, i , and its value varies between 0 and 1. Accuracy
 417 factor value represents the measure of closeness of that input parameter value with the
 418 most favourable value range; w_i represents the weightage function of the input
 419 parameter, i , and its value varies between 0 and 1. This weightage factor represents the
 420 relative importance of that input parameter influencing the output parameter.

421 In calculation of selection score for present in-situ MEOR technique, the
 422 weightage factor, w_i , of different input parameters, i , are same as the RI score of
 423 different input parameters as shown in Fig. 5a. Hence, based on the determined
 424 weightage factor (*i.e.*, RI score) for all the 13 input parameters, the selection score for
 425 the in-situ MEOR technique shall be calculated by using Eq. (12).

$$\begin{aligned}
 426 \quad Selection\ Score = & 0.168 a_{Yps} + 0.146 a_{Sori} + 0.14 a_u + 0.125 a_{\mu w} + 0.114 a_{Ai} + \\
 427 \quad & 0.1 a_{Yxs} + 0.08 a_{Si} + 0.047 a_{Umax} + 0.02 a_{Tr} + 0.018 a_{Swir} + \\
 428 \quad & 0.016 a_{Xi} + 0.014 a_{Kxs} + 0.012 a_{\sigma i} \quad (12)
 \end{aligned}$$

429 The value of accuracy factor values of each input parameter (a_i) are determined from
 430 lab experiments. The value of a_i varies case-to-case basis, and its value depends on the
 431 nature of reservoir and microbe-nutrient pair used and the operational conditions
 432 adopted. Upon calculation of a_i from initial experiments, the selection score for in-situ
 433 MEOR technique shall be quickly calculated using Eq. (12), which will subsequently
 434 help to screen the suitability of in-situ MEOR technique among other EOR techniques

435 for field implementation at the initial laboratory investigation itself. In addition to it, the
436 selection score presented in Eq. (12) also helps to identify the suitable microbe-nutrient
437 combination among several available combinations for attaining better oil recovery at
438 the initial laboratory investigation itself. The microbe-nutrient combination that have
439 highest selection score value will recover relatively more oil from the reservoir for a
440 given reservoir and operational conditions. Thus, it is concluded that the RI score
441 determined from feature importance study in present PIML approach will: (a) help to
442 screen the suitability of in-situ MEOR technique among other EOR techniques for field
443 implementation; and also (b) helps to screen the suitable microbe-nutrient combination
444 for successful implementation of in-situ MEOR technique in the field at the initial
445 laboratory investigation itself.

446 ***3.5 Application of different ML algorithms in the PIML approach to predict the oil*** 447 ***recovery performance of in-situ MEOR technique***

448 [Figure 6]

449 Figure 6 shows the oil recovery (in %) predicted by different ML models used in
450 the PIML approach against the benchmark (actual) results which are obtained from
451 physics-based models. The most accurate ML model with better prediction capability
452 will have the scatter plot points lying closer to the line equation $y' = x$ (here, y' and x
453 are benchmark and predicted values, respectively), and correspondingly will have R^2
454 and $RMSE$ value closer to 1 and 0, respectively. While, for the ML model with least
455 accuracy, the scatter plot points are spread widely from the line equation $y' = x$, and it
456 will also have relatively lower R^2 and relatively higher $RMSE$ value. The R^2 , $RMSE$ and
457 EVS values of all the 12 ML algorithms that were used in the present PIML approach
458 study is presented in Table 2.

[Table 2]

459
460 Based on the results presented in Fig. 6 and Tab. 2, it is inferred that among all
461 the 12 ML algorithms/models that are used in the present PIML approach, Neural
462 Networks ML model had performed better in predicting the output oil recovery ($R^2 =$
463 0.9873 , $RMSE = 0.7145$). The neural networks ML algorithm/model outperforms other
464 ML algorithms in prediction because it can implicitly detect complex non-linear
465 relationships between dependent and independent variables, and it also have the ability
466 to detect all possible interactions between the input variables. Followed by the neural
467 network model, it is observed that the Support Vector Regression (SVR) is the second-
468 best ML model that can better predict the oil recovery ($R^2 = 0.9644$; $RMSE = 1.184$).
469 The main advantage of SVR model is that it is less susceptible to outliers than other
470 data-driven models but it's harder to manually tune hyperparameters. Next to SVR
471 algorithm, it is found that the 4th degree Polynomial Regression model had predicted the
472 oil recovery better ($R^2 = 0.963$; $RMSE = 1.26$) as it has the ability to better map the
473 non-linear relationship between the input and output variables. Amongst all the 12 ML
474 models that were used in the present PIML approach for oil recovery prediction, it is
475 found that K-Nearest Neighbours ML model is the least accurate model ($R^2 = 0.3698$;
476 $RMSE = 3.369$). Thus, from the present study, it is concluded that to predict the oil
477 recovery performance of in-situ MEOR technique at initial lab stage, the Neural
478 Network is the best ML algorithm that need to be used in the PIML approach.

479 ***3.5 Case study on application of PIML approach for screening of suitable microbe-*** 480 ***nutrient combination for in-situ MEOR implementation***

481 To illustrate the application of present PIML approach on screening of suitable
482 microbe-nutrient combination, a case study using synthetic data has been carried out.

[Table 3]

483
484 Table. 3 presents the microbial kinetic parameters for 4 different combinations of
485 microbes and nutrients, and rest all other parameters are kept constants. By feeding the
486 inputs through the trained neural network ML algorithm, the output oil recovery is
487 calculated and presented in the last column of Tab 3. It is inferred from Tab.3 that
488 among all the available combinations, the combination 4 shows highest oil recovery,
489 hence that corresponding microbe-nutrient pair can be used for field implementation.

490

491 **4. Conclusions**

492 Physics-Informed Machine Learning (PIML) approach is adopted to investigate
493 the performance of in-situ MEOR technique from limited experimental data, which is
494 difficult with conventional experimental and modelling approaches. Neural network ML
495 model used in the PIML approach had more accurately predicted the oil recovery. Y_{PS} ,
496 flow velocity and initial oil saturation (S_{ori}) are correspondingly the most influential
497 microbial kinetic, operational and reservoir parameter. Higher oil recovery is achieved
498 by selecting a microbe-nutrient-reservoir pair having higher Y_{PS}/Y_{XS} and S_{ori} values.
499 This PIML approach helps to screen/identify suitable microbe-nutrient-reservoir pair at
500 initial laboratory stage itself, ensuring its success during the field implementation.

501 **Funding Source:** This research did not receive any specific grant from funding
502 agencies in the public, commercial, or not-for-profit sectors.

503 **References**

504 1. Ansah, E.O., Thanh, H.V., Sugai, Y., Nguele, R., Sasaki, K., 2020. Microbe-induced
505 fluid viscosity variation: field-scale simulation, sensitivity and geological uncertainty. *J*
506 *Petrol. Explor. Prod. Technol.* 10, 1983–2003.

507 2. Cruz, I.A., Chuenchart, W., Long, F., Surendra, K.C., Andrade, L.R.S., Bilal, M.,
508 Figueiredo, R.T., Khanal, S.K., Ferreira, L.F.R., 2021. Application of machine learning
509 in anaerobic digestion: Perspectives and challenges. *Bioresour. Technol.* 126433.

510 3. Joshi, S.J., Al-Wahaibi, Y.M., Al-Bahry, S.N., Elshafie, A.E., Al-Bemani, A.S., Al-
511 Bahry, A., Al-Mandhari, M.S., 2016. Production, characterization, and application of
512 *bacillus licheniformis* W16 biosurfactant in enhancing oil recovery. *Front. Microbiol.* 7,
513 1853.

514 4. Jeong, M.S., Lee, Y.W., Lee, H.S., Lee, K.S., 2021. Simulation-Based Optimization
515 of Microbial Enhanced Oil Recovery with a Model Integrating Temperature, Pressure,
516 and Salinity Effects. *Energies*, 14, 1131.

517 5. Jeong, M.S., Cho, J., Lee, K.S., 2022. Systematic modelling incorporating
518 temperature, pressure, and salinity effects on in-situ microbial selective plugging for
519 enhanced oil recovery in a multi-layered system, *Biochem. Eng. J.* 177, 108260.

520 6. Karniadakis, G.E., Kevrekidis, I.G., Lu, L., Perdikaris, P., Wang, S., Yang, L.,
521 2021. Physics-informed machine learning. *Nat. Rev. Phys.* 4, 422-440.

522 7. Keprate, A., Ratnayake, R.M.C., 2019. Data Mining for Estimating Fatigue Strength
523 Based on Composition and Process Parameters. *Proc. ASME 2019 38th Int. Con. on*
524 *Ocean, Offshore and Arctic Eng. Vol 4: Materials Technology.*

525 8. Liu, H., Zhang, J., Liang, F., Temizel, C., Basri, M.A., Mesdour, R., 2021.
526 Incorporation of physics into machine learning for production prediction from

527 unconventional reservoirs: a brief review of the gray-box approach. SPE Res. Eval.
528 Eng. 24, 847–858.

529 9. Markande, A.N., Patel, D., Varjani, S.J., 2021. A review on biosurfactants:
530 properties, applications and current developments. Bioresour. Technol. 330, 124963.

531 10. Nielsen, S.M., Nesterov, I., Shapiro, A.A., 2016. Microbial enhanced oil recovery-a
532 modeling study of the potential of spore-forming bacteria. Comput. Geosci. 20, 580.

533 11. Nikolova, C., Gutierrez, T., 2020. Use of microorganisms in the recovery of oil
534 from recalcitrant oil reservoirs: current state of knowledge, technological advances and
535 future prespective. Front. Microbiol. 10, 2996.

536 12. Sivasankar, P., Kanna, R., Kumar, G.S., Gummadi, S.N., 2016. Numerical
537 modelling of biophysicochemical effects on multispecies reactive transport in porous
538 media involving *Pseudomonas putida* for potential microbial enhanced oil recovery
539 application. Bioresour. Technol. 211, 348-359.

540 13. Sivasankar, P., Kumar, G.S., 2017. Influence of pH on dynamics of microbial
541 enhanced oil recovery processes using biosurfactant produced *Pseudomonas putida*:
542 Mathematical modelling and numerical simulation. Bioresour. Technol. 224, 498-508.

543 14. Shibulal, B., Al-Bahry, S.N., Al-Wahaibi, Y.M., Elshafie, A.E., Al-Bemani, A.S.,
544 Joshi, S.J., 2018. Microbial-Enhanced Heavy Oil Recovery under Laboratory
545 Conditions by *Bacillus firmus* BG4 and *Bacillus halodurans* BG5 Isolated from Heavy
546 Oil Fields. Colloids Interfaces. 2, 1.

547 15. Sivasankar, P., Kumar, G.S., 2019. Influence of bio-clogging induced formation
548 damage on performance of microbial enhanced oil recovery processes. Fuel. 236, 109.

- 549 16. Thanh, H.V., Sugai, Y., Sasaki, K., 2020. Application of artificial neural network
550 for predicting the performance of CO₂ enhanced oil recovery and storage in residual oil
551 zones. *Sci. Rep.* 10, 18204.
- 552 17. Tang, Q., Chen, Y., Yang, H., Liu, M., Xiao, H., Wang, S., Chen, H., Naqvi, S.R.,
553 2021. Machine learning prediction of pyrolytic gas yield and compositions with feature
554 reduction methods: Effects of pyrolysis conditions and biomass characteristics.
555 *Bioresour. Technol.* 339, 125581.
- 556 18. Varjani, S.J., Upasani, V.N., 2016. Core Flood study for enhanced oil recovery
557 through ex-situ bioaugmentation with thermo- and halo-tolerant rhamnolipid produced
558 by *Pseudomonas aeruginosa* NCIM 5514. *Bioresour. Technol.* 220, 175-182.
- 559 19. Varjani, S.J., Upasani, V.N., 2017. Critical review on biosurfactant analysis,
560 purification and characterization using rhamnolipid as a model biosurfactant. *Bioresour.*
561 *Technol.* 232, 389-397.
- 562 20. Wang, Z., Peng, X., Xia, A., Shah, A.A., Huang, Y., Zhu, X., Zhu, X., Liao, Q.,
563 2022. The role of machine learning to boost the bioenergy and biofuels conversion.
564 *Bioresour. Technol.* 343, 126099.
- 565 21. Zhang, W, Li, J., Liu, T., Leng, S., Yang, L., Peng, H., Jiang, S., Zhou, W., Leng,
566 L., Li, H., 2021. Machine learning prediction and optimization of bio-oil production
567 from hydrothermal liquefaction of algae. *Bioresour. Technol.* 342, 126011.

568

569

570

571

572

573

574

575

576

577

578

579

580

581

582 **Figures Caption**

583 1. Procedure of PIML approach followed in the present study to predict oil recovery by
584 in-situ MEOR process

585 2. Frequency distribution of input and output data that are generated and used for
586 training and testing of ML algorithms in the PIML approach

587 3. Validation of present microbial kinetic model results with measured experimental
588 data for (a) variation of microbial concentration with time, (b) variation of sucrose
589 concentration with time, (c) variation of biosurfactant concentration with time

590 4. (a) Pearson correlation and Spearman correlation coefficient matrix for microbe,
 591 operational, reservoir and % oil recovery data, (b) Correlation coefficient values for
 592 input microbe, operational and reservoir data towards output % oil recovery

593 5. (a) Relative Importance (RI) score of all input parameters, (b) RI score of input
 594 microbial-nutrient parameters, (c) RI score of input operational parameters, (d) RI score
 595 of input reservoir parameter in predicting output % of oil recovery

596 6. Comparative performance of 12 different ML algorithms in predicting the oil
 597 recovery against the actual % of oil recovery for in-situ MEOR application.

598 **Tables Caption**

599 1. Input parameters and their corresponding value range used in the present study

600 2. Performance of different ML algorithms in predicting the actual % of oil recovery

601 3. Microbial kinetic parameters for different microbial-nutrient combinations and their
 602 corresponding oil recovery determined using PIML modelling approach.

603 Table 1. Input parameters and their corresponding value range used in the present study
 604 [Sivasankar et al. (2016)]

Parameter	Reference value	Range
Y_{XS}	0.1843	0.092 - 0.276
Y_{PS}	0.078 [Sivasankar et al. (2016)]	0.03900733 - 0.116996715
K_{XS} (g/l)	6.86 [Sivasankar et al. (2016)]	3.430058808 - 10.28959695
U_{max} (h^{-1})	0.053 [Sivasankar et al. (2016)]	0.02650387 - 0.079495509

X_i (g/l)	0.1521167 [Sivasankar et al. (2016)]	0.076094593 - 0.22824074
S_i (g/l)	19.234 [Sivasankar et al. (2016)]	9.617601084 - 28.84936382
A_i (g/l)	3 [Sivasankar et al. (2016)]	1.500165456 - 4.49988547
T_r (h)	150	100 – 200
u_w (m/h)	0.0004 [Sivasankar et al. (2016)]	0.0002 – 0.0006
μ_w (Nhm ⁻²)	0.001 [Sivasankar et al. (2016)]	0.0005 – 0.0015
Initial IFT (mN/m)	51.6 [Sivasankar et al. (2016)]	25.80405697 - 77.39695
S_{wir}	0.2	0.10000517 - 0.299989777
S_{ori}	0.4	0.20000454 - 0.599986979
Output - % oil recovery	Mean - 7.423469637 Median - 5.510703244	0.174742622 - 48.23409386

605
606
607

608 Table 2: Performance of different ML algorithms in predicting the actual % of oil
609 recovery

Model	R^2	RMSE	Explained Variance Score
KNN	0.369897442	3.369742385	0.370031425
Decision Trees	0.408587985	4.356687642	0.408683171
Lasso	0.510880307	3.697724477	0.51138261
Ridge	0.512474691	3.697351147	0.512976983

Linear Regression	0.51299017	3.697264614	0.513491055
Random Forests	0.639724278	2.941482946	0.63972701
ADA Boost	0.639746354	2.811959461	0.639980378
Gradient Boosting	0.896025654	1.851540808	0.896025658
Gaussian Process	0.951787039	1.353896887	0.951802595
Polynomial (4)	0.963022723	1.26029449	0.963039744
SVR	0.964436929	1.184682456	0.964596291
Neural Network	0.987349995	0.714597767	0.987656577

610

611

612

613

614

615

616

617

618

619 Table 3: Microbial kinetic parameters for different microbial-nutrient combinations and

620 their corresponding oil recovery determined using PIML modelling approach

621

Combinations	Y_{XS}	Y_{PS}	K_{XS}	U_{max}	Output Oil Recovery, %
1	0.098734	0.067978	4.077158	0.068247	6.3529167
2	0.148067	0.081408	4.763728	0.056552	4.531987

3	0.169445	0.091877	4.923773	0.053963	4.549041
4	0.121985	0.095722	8.262717	0.038336	7.3623314

622

623

624

625

626

627

628

629

630

631

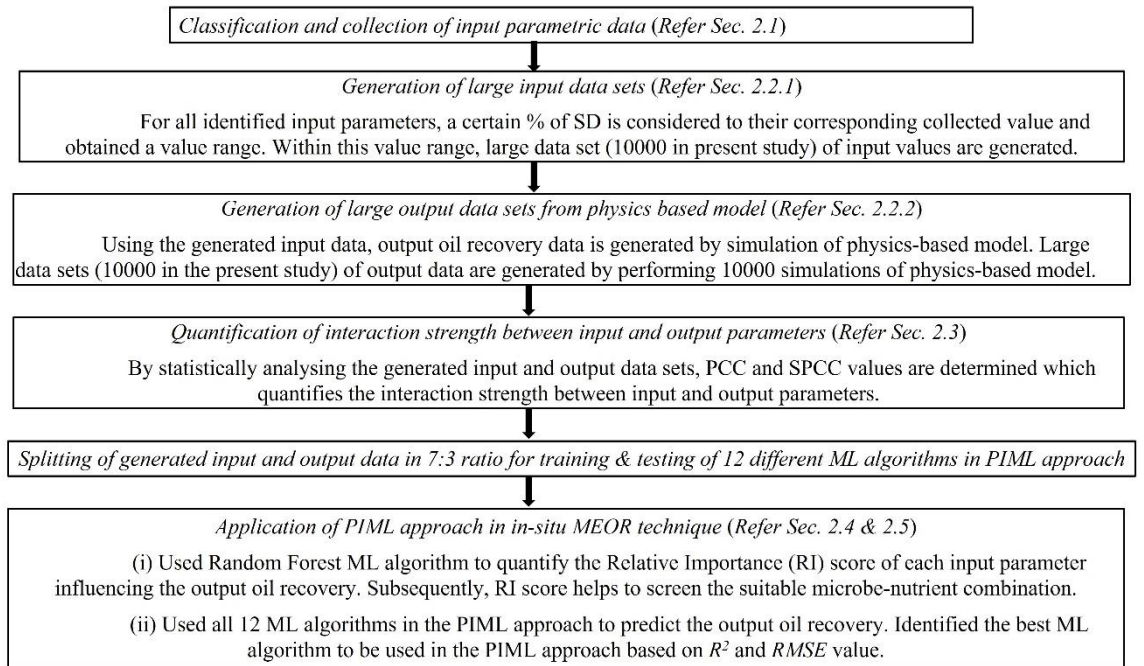
632

633

634

635

636



637

638 **Figure 1:** Procedure of PIML approach followed in the present study to predict oil

639 recovery by in-situ MEOR process (NIKHIL WILL CHANGE IT)

640

641

642

643

644

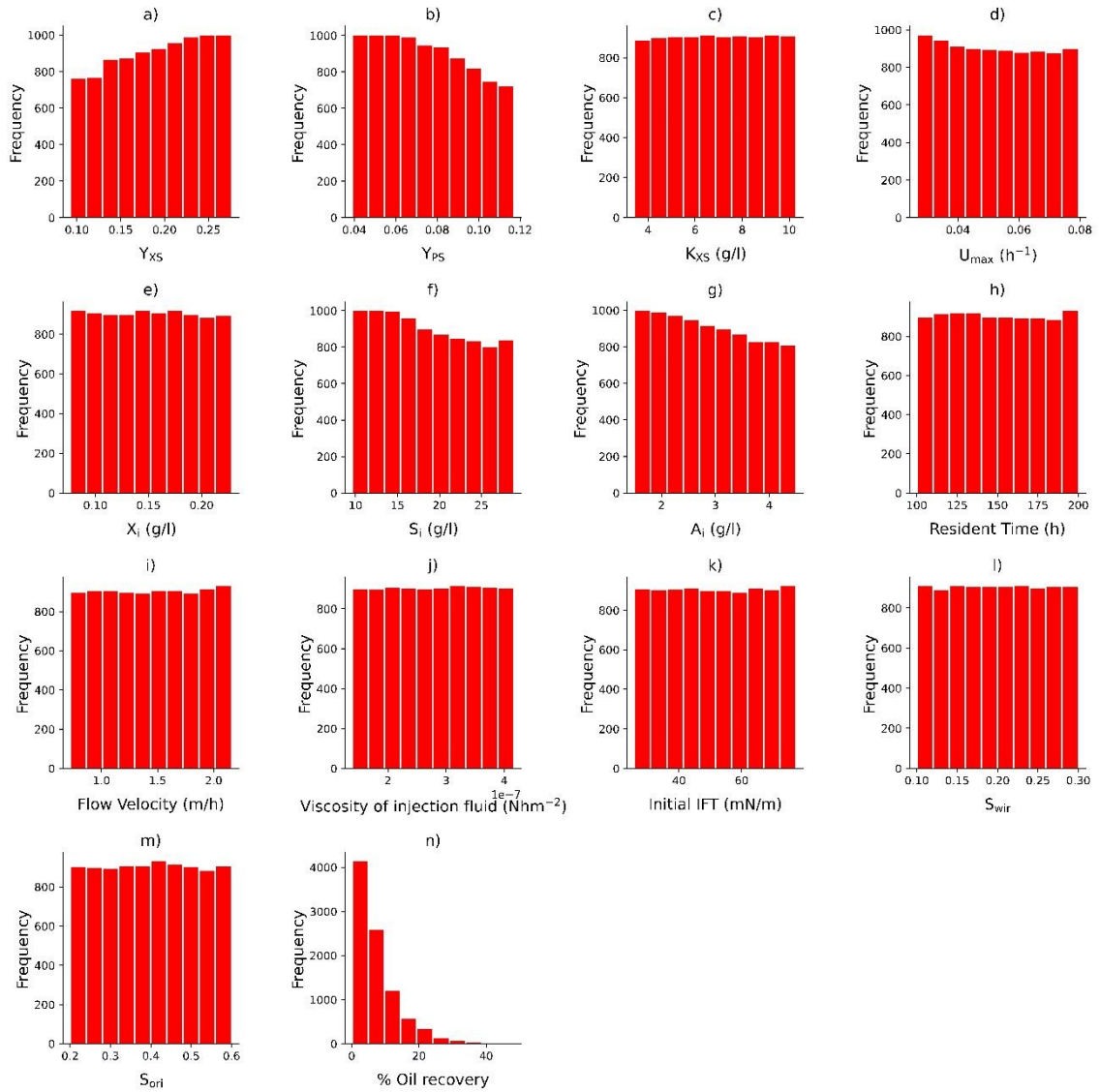
645

646

647

648

649



650

651 **Figure 2:** Histogram of input and output data that are generated and used for training

652 and testing of ML algorithms in the PIML approach.

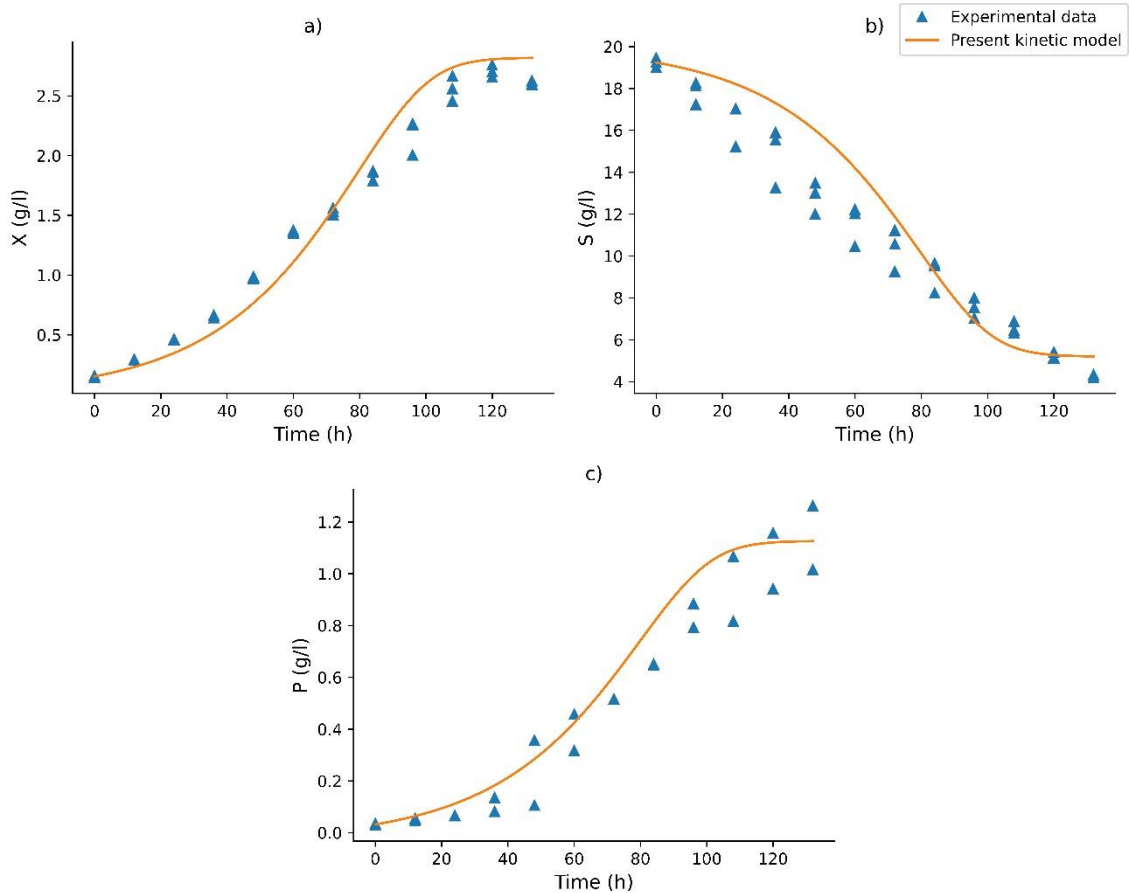
653

654

655

656

657



658

659 **Figure 3:** Validation of present microbial kinetic model results with measured
 660 experimental data for (a) variation of microbial concentration with time, (b) variation of
 661 sucrose concentration with time, (c) variation of biosurfactant concentration with time.

662

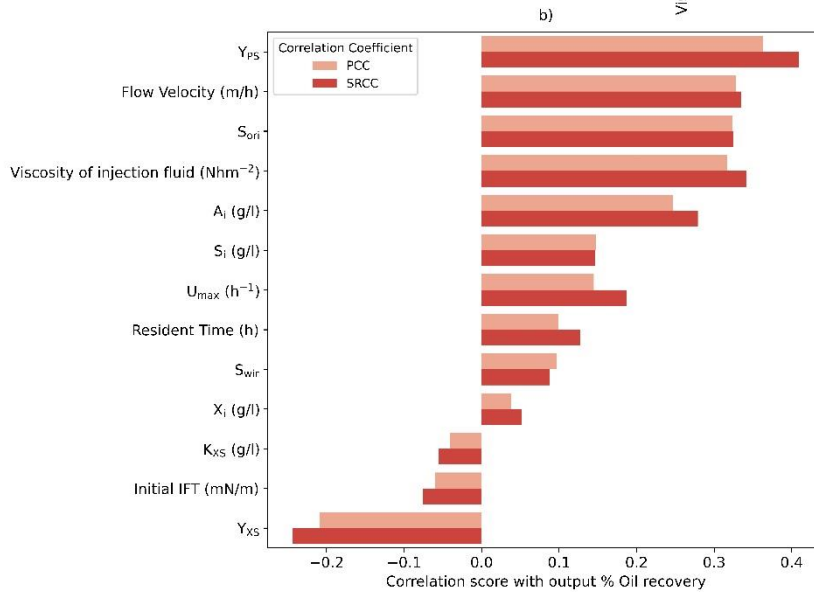
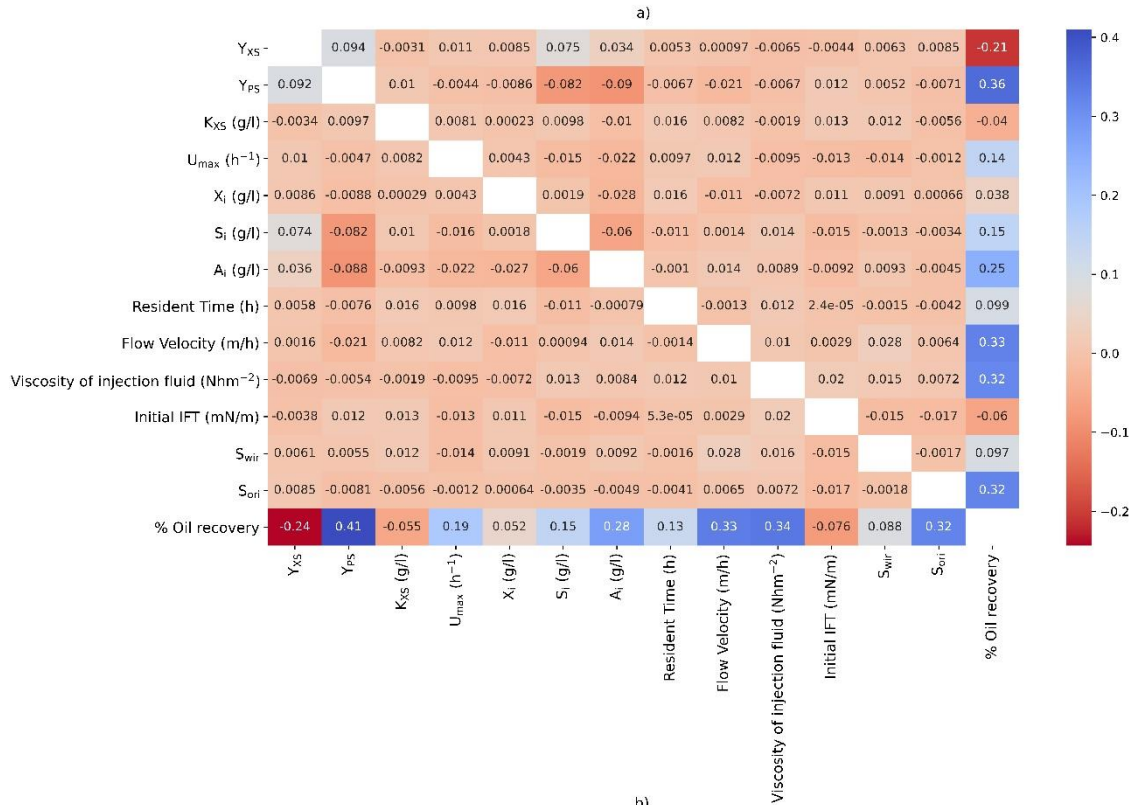
663

664

665

666

667



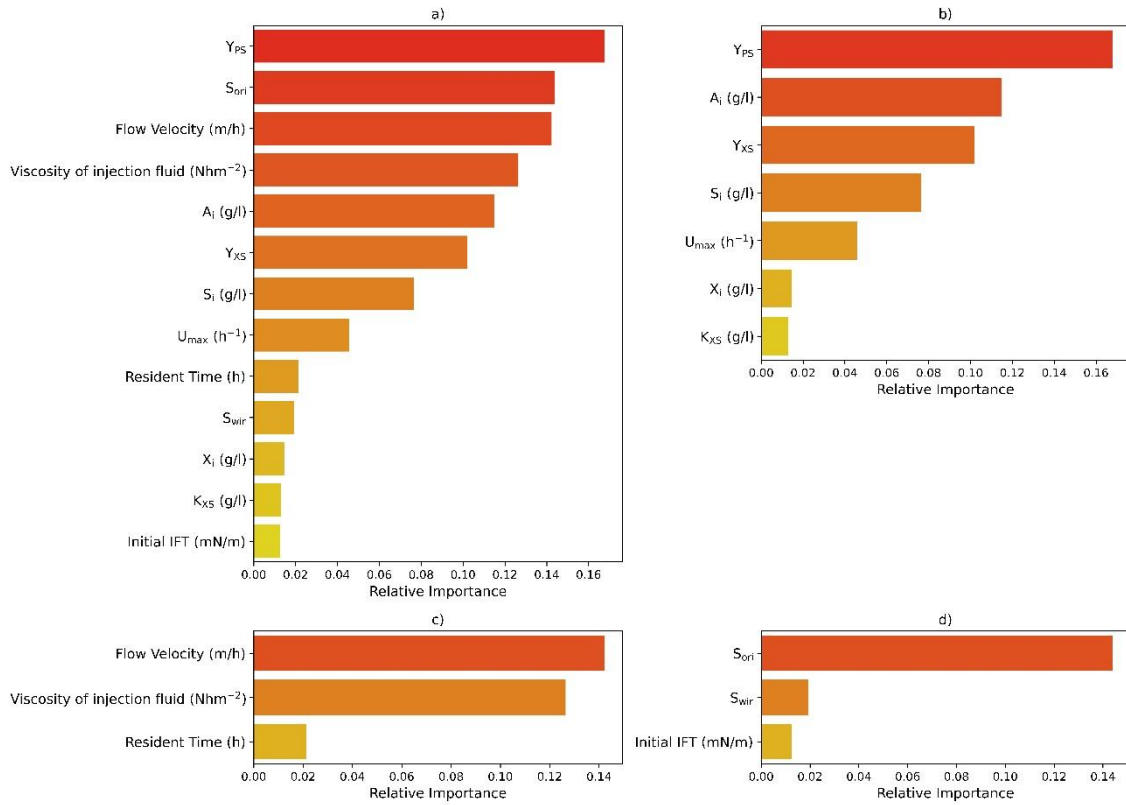
668

669 **Figure 4:** (a) Pearson correlation and Spearman correlation coefficient matrix for

670 microbe, operational, reservoir and % oil recovery data, (b) Correlation coefficient

671 values for input microbe, operational and reservoir data towards output % oil recovery.

672



673

674 **Figure 5:** (a) Relative Importance (RI) score of all input parameters, (b) RI score of
 675 input microbial-nutrient parameters, (c) RI score of input operational parameters, (d) RI
 676 score of input reservoir parameter in predicting output % of oil recovery.

677

678

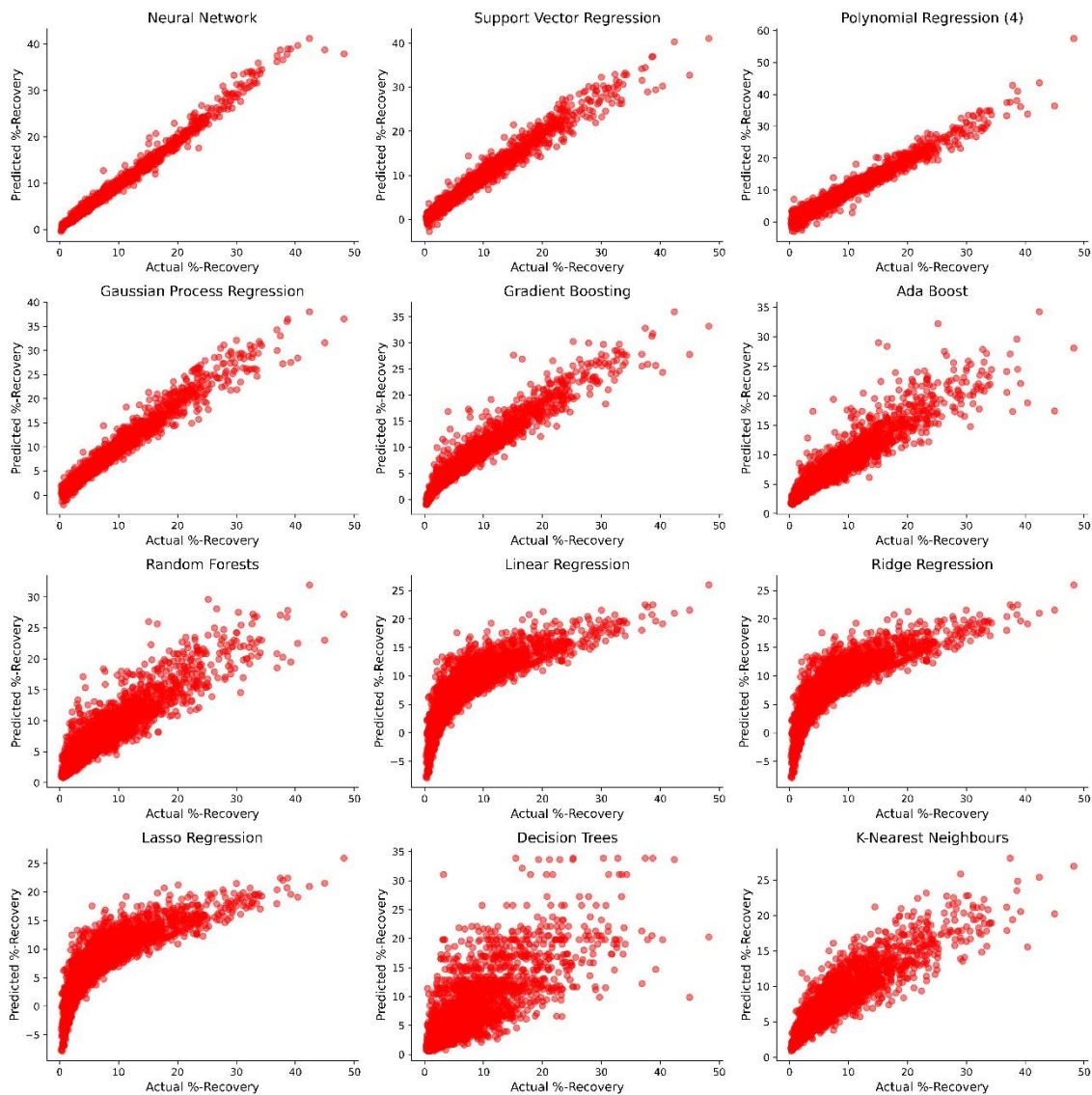
679

680

681

682

683



684

685 **Figure 6:** Comparative performance of 12 different ML algorithms in predicting the oil
 686 recovery against the actual % of oil recovery for in-situ MEOR application.

687